INSTITUTE OF PHYSICS PUBLISHING JOURNAL OF PHYSICS D: APPLIED PHYSICS

J. Phys. D: Appl. Phys. **35** (2002) 1821–1827 PII: S0022-3727(02)36411-8

Structural and magnetic characterization of single-crystalline Fe/MgO/Fe magneto-tunnel junctions grown on GaAs(001) and InP(001)

M Przybylski[1,2,3], J Grabowski[1,2], F Zavaliche[1], W Wulfhekel[1], R Scholz[1] and J Kirschner[1]

[1] Max-Planck-Institut fur Mikrostrukturphysik, Weinberg 2, 06120 Halle, Germany
[2] Solid State Physics Department, Faculty of Physics and Nuclear Techniques, University of Mining and Metallurgy, 30-059 Krakow, Poland

E-mail: mprzybyl@mpi-halle.de

Received 1 May 2002
Published 16 July 2002
Online at stacks.iop.org/JPhysD/35/1821

Abstract

We report on the structural and magnetic characterization of Ni/Fe/MgO/Fe structures grown on GaAs(001) and InP(001). High-resolution transmission electron microscopy images confirm a good crystallographic order of the structures grown on GaAs(001). On the contrary, the structures grown on InP(001) do not show any long-range crystallographic order. For structures grown on GaAs(001), magneto optic Kerr effect analysis shows steps in the hysteresis loops corresponding to magnetization reversal processes that occur independently in both ferromagnetic (FM) films. No FM coupling between the bottom Fe and the top Ni/Fe films is detected. The coercivity of the bottom Fe film in the junction is increased in comparison to the Fe/GaAs(001) film of the same thickness most likely due to crystallographic defects. The defects are created in the top Ni/Fe bilayer and are spread over the whole single-crystalline structure. For structures grown on InP(001), a strong FM coupling is deduced from the hysteresis loops and is interpreted in terms of the orange-peel coupling.

1. Introduction

Metal-based ferromagnetic (FM) spin-aligners, which operate at weak magnetic fields and room temperature (RT), remain a subject of great interest, in particular when grown on semiconducting (SC) substrate. Unfortunately, the up to date experiments of spin injection directly from the metal-FM into the SC have only shown effects of less than 2% [1], in agreement with theoretical predictions for diffusive electron transport between two materials of very different conductivity [2]. Recent theoretical works predict that the efficiency of the spin injection from a FM into a SC can be improved for electrons created by tunnelling through an insulating (I) barrier since such a process is not affected by the conductivity mismatch and results in the conservation of the spin polarization [3]. Recently the prediction was experimentally confirmed [4]. Another possibility is spin injection across FM/SC interfaces in the ballistic regime with the probability determined by the difference between the spin conduction sub-bands of the FM and the conduction band of the SC [5]. And, finally, spin-polarized hot electrons (of energies higher than E_F) can be injected into the SC [6]. If this is realized by tunnelling between two FM layers, the spin polarization of the states available for tunnelling comes into play, i.e. the FM/I/FM structure exhibits tunnelling magnetoresistance (TMR). The TMR of an epitaxial Fe/MgO/Fe(001) junction was calculated and a large effect (of 1000% for a perfect interface and 76% for a Fe–O interface layer) is predicted theoretically [7, 8] (and recently experimentally confirmed with the TMR value of 60% at 30 K [9]). Additionally, for the

[3] Author to whom correspondence should be addressed.

tunnelling electrons, a barrier to enter the SC is introduced, which is spin dependent due to the largely different mean free paths for majority and minority carriers. To achieve the effect of spin-dependent current injection into the SC, the thickness of the intermediate FM layer should scale with the inelastic mean free path of spin-up or spin-down electrons. The resulting ballistic electron current can be more than 90% polarized [10].

It is obvious that the transport properties of FM/I/FM junctions depend on the relative orientation of magnetization in FM layers. In order to operate the junction, i.e. to switch the magnetization of both FM films independently, one of the films must be magnetically softer. The switching behaviour of the soft FM film and the magnetic properties of the hard FM film can influence each other [11]. The tunnelling barrier minimizes magnetic coupling between the FM films, but interactions between them may still be present. First of all, the presence of any metallic 'bridges' through the insulating barrier will be reflected both in FM coupling and in the transport properties. Secondly, magnetostatic orange-peel coupling occurs between the films due to correlated roughness and due to the magnetic stray fields of the domain walls in the two FM films [11]. In the case of the epitaxially grown junctions, strains due to the lattice mismatch between the growing materials can also play a significant role. In particular, the strain can influence the coercivity of both FM films making the independent switching of their magnetization more or less preferable. The coupling properties can be engineered to meet the application requirements. This concerns the interface quality and continuity of the insulating layer/barrier, as well as determination of the total magnetic moment of one FM film with respect to the other. The magnetic coupling between the films should be low enough to allow the independent switching of their magnetization.

In this paper, we report on the structural and magnetic characterization of Ni/Fe/MgO/Fe structures grown on GaAs(001) and InP(001). The main emphasis is put on the influence of the 'layer design' and crystallographic quality of the junctions on their magnetic properties.

2. Experimental

The sample preparation and characterization were carried out in an ultra-high vacuum (UHV) multichamber system equipped with molecular beam epitaxy (MBE), Auger electron spectroscopy (AES), low energy electron diffraction (LEED), scanning tunnelling microscopy (STM) and *in situ* longitudinal magneto optic Kerr effect (MOKE). MOKE loops were collected in the longitudinal geometry using an electromagnet with a maximum field of 300 Oe, and intensity stabilized laser diode (wavelength 670 nm).

The InP and GaAs substrates were cleaned by 500 eV Ar^+ sputtering at 290°C and 590°C, respectively. After the cleaning procedures were completed, no traces of contamination were detected in AES spectra and sharp LEED patterns were observed. For InP(001), a P-rich (2×4) reconstruction was obtained, which is known to prevent the formation of magnetically dead layers at the interface with Fe [11]. For the GaAs(001) substrate, the cleaning procedure resulted in a Ga-terminated (4×6)-like reconstruction, which is found to protect the Fe film against strong intermixing with As and Ga [13, 14].

Fe, Ni, MgO and Au were deposited at a rate of 1–1.5 ML min^{-1} by electron beam evaporation from thoroughly outgassed high-purity Fe, Ni and MgO rods, as well as from a Mo crucible filled with Au. The growth was carried out at RT at a pressure between 2×10^{-10} and 6×10^{-10} mbar (maximum pressure after a long deposition of Ni).

3. Results

For both substrates, the Fe films grown at RT were magnetized in-plane. In-plane measurement showed a dominant uniaxial in-plane magnetic anisotropy with the easy-axis along [−110] and [110] in the Fe films grown on InP(001) and GaAs(001), respectively [12–15]. We note that in our previous paper [15], the orientation of the easy-axis in the Fe films grown on GaAs(001) was erroneously described as oriented along the [−110] direction. To achieve the growth of a single crystalline magneto-tunnel junction, we used MgO as the tunnelling barrier [16]. In this paper, a MgO film of thickness varying between 10 and 20 ML was grown epitaxially on 14 ML of Fe previously deposited on InP(001) or GaAs(001), without any buffer layer. The observed LEED patterns exhibiting a four-fold symmetry confirm a good crystallographic order in the Fe and MgO films grown on GaAs(001). After the preparation of the MgO film, a second Fe film was deposited at RT, whose LEED pattern was of reasonable quality [15]. Eventually, in order to protect the Fe/MgO/Fe structure against oxidation, the samples were covered with about 30 ML of Au. We repeated exactly the same procedure for the growth of Fe/MgO/Fe magneto-tunnel structure on InP(001). However, no LEED patterns were seen after the growth of any film of the structure [12]. In our opinion, this is caused by the structural disorder in the bottom Fe film. This disordered layer might affect the epitaxial growth of the further films building up the junction. High-resolution transmission electron microscopy (TEM) images confirm a good crystallographic order in the first Fe and MgO films as well as in the Au-cover layer of the structures grown on GaAs(001) (figure 1(*a*)). On the contrary, the structures grown on InP(001) do not show any long-range crystallographic order (figure 1(*b*)). The InP/Fe interface region is polycrystalline or possibly amorphous which influences the further growth of Fe, MgO and other films building up the structure, and explains the lack of LEED pattern after any film of the structure is grown.

Concerning magnetic properties, the most important for the junction operation is to orient the magnetization of FM films anti-parallel at clearly defined ranges of applied magnetic field. For a better definition of the coercive fields in the two Fe films, the top layer was made harder by reducing its thickness and adding Ni, that is known to grow epitaxially on Fe(001) [15,17]. The first several monolayers follow the bcc-stacking with the same lateral spacing as it is observed for Fe(001) [17]. After reaching the critical thickness of about 5 ML, the Ni overlayer transforms into a more complicated structure. The resulting Fe/Ni bilayer shows remarkable magnetic properties like four-fold anisotropies far exceeding those observed in bulk Fe [17].

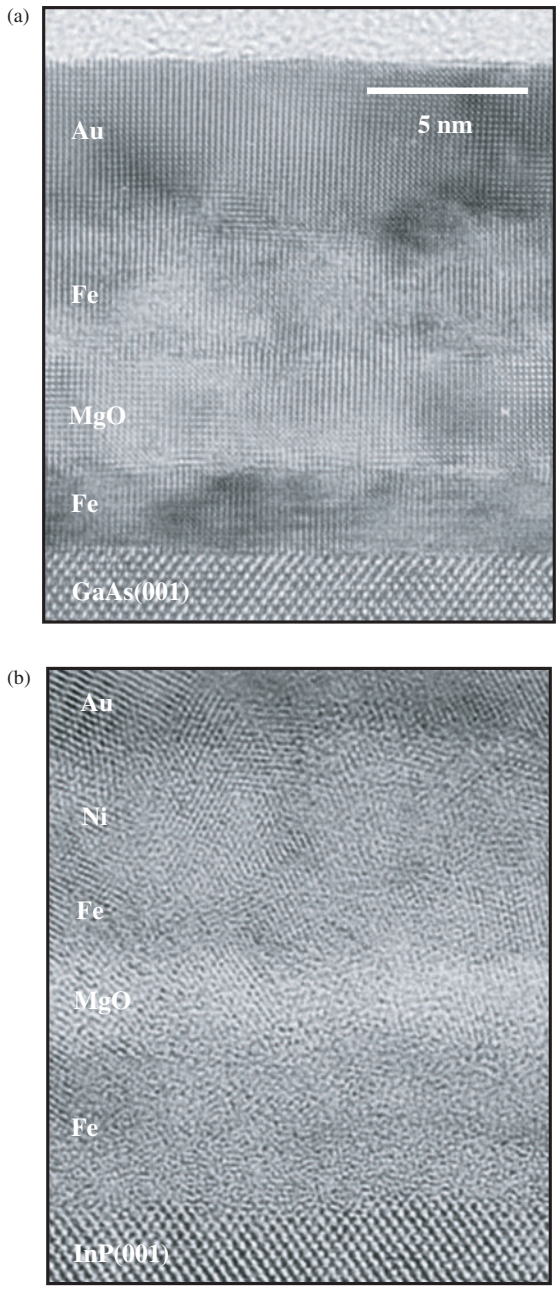

Figure 1. High-resolution TEM images over the cross-sections of: (*a*) 30 ML Au/20 ML Fe/15 ML MgO/14 ML Fe/GaAs(001) and (*b*) 20 ML Au/20 ML Ni/10 ML Fe/10 ML MgO/20 ML Fe/InP(001) magneto-tunnel junctions. The images confirm a good crystallographic order of the structures grown on GaAs(001). The structures grown on InP(001) do not show any long-range crystallographic order.

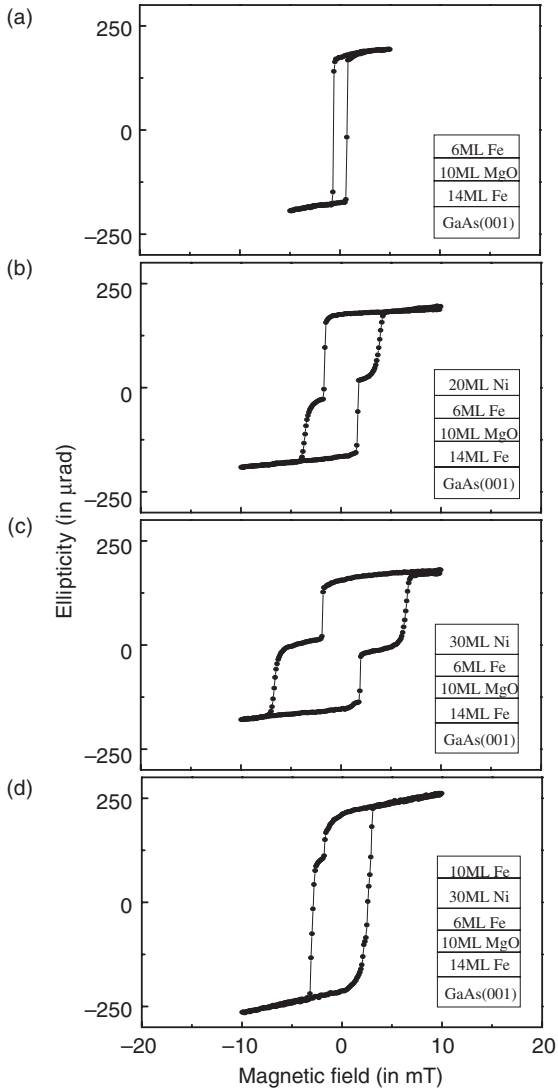

Figure 2. MOKE loops measured at RT along the [110] direction for 6 ML Fe/10 ML MgO/14 ML Fe/GaAs(001) (*a*), then covered with 20 ML of Ni (*b*), and 30 ML of Ni (*c*). The loops evolve with adding Ni showing a remarkably increased coercivity in the top FM film. Covering with additional Fe decreases the coercivity of the top FM film as it is seen from the loop measured after covering 30 ML Ni/6 ML Fe/10 ML MgO/14 ML Fe/GaAs(001) with 10 ML of Fe (figure 2(*d*)).

In particular, the thickness of Fe and Ni layers contributing to the top FM film was chosen with respect to the thickness of the bottom Fe film (14 ML) in order to get a nearly zero net magnetization for an anti-parallel orientation of the two magnetic electrodes. The resulting MOKE loops of Fe/MgO/Fe on GaAs(001) before adding Ni (figure 2(*a*)) and with two characteristic magnetization jumps after adding Ni are shown in the figures 2(*b*) and (*c*). By comparison with the MOKE loop of a single Fe layer showing only one jump, and due to its evaluation with adding Ni (that concerns both changing coercivity and magnetization), one can conclude that each jump is related to the switching of magnetization of one of the two FM layers. The low field jumps in the Kerr signal are associated with the magnetization reversal in the bottom Fe layer of the structure. The observed coercivity of the bottom layer in Fe/MgO/Fe structure is similar to that of a bare Fe layer on GaAs. Upon adding Ni, the coercivity to switch the top layer increases significantly. The coercivity of the bottom layer, however, in the presence of the FM top Ni/Fe film is often increased in comparison to the coercivity of the Fe/GaAs(001) film of the same thickness. This increase may be related to a FM coupling between the two FM layers separated by MgO or to any other mechanism by which the top FM film influences the coercivity of the bottom one. The net ellipticity close to zero (after covering 6 ML of Fe with 30 ML

of Ni; figure 2(*c*)) clearly confirms that the steps in the MOKE loop correspond to magnetization reversal processes that occur independently in both FM films. The loop (figure 2(*c*)) shows a remarkably increased coercivity in the top film. Note that covering the top Ni/Fe film with additional Fe (the loop shown in figure 2(*d*)) results in increasing that part of magnetic moments that is rotated at a higher field, and thus is confirmed to correspond to the top FM film. In addition, covering with 10 ML of Fe clearly decreases the coercivity of the top film. This suggests that the transition to the transformed-bcc-Ni [17] is partially reversed to a bcc-stacking of Ni atoms that is forced by the covering Fe layer. This is in agreement with our previous observation of the Fe-overlayer induced bcc-stacking in the Ni film grown on GaAs(001) [14].

Any change of Fe thickness in the top Ni/Fe FM bilayer results in a change of the net magnetization of the sample, and in the coercivity of the top FM film. As expected, the thicker the Fe film, the less pronounced the influence of the covering Ni layer is on the coercivity (for the same thickness of MgO). This is depicted in figure 3 for Ni/6 ML Fe/MgO/Fe/GaAs(001) and Ni/10 ML Fe/MgO/Fe/GaAs(001) structures. Covering with 20 ML of Ni changes the coercivity of the top 6 ML thick Fe film by about 2.5 mT, whereas in the case of a 10 ML thick Fe film this change is about 1.5 mT. Even for Ni thickness of up to 30 ML, the coercivity increases up to 6 mT in the case of 6 ML of Fe, but only up to 4 mT in the case of 10 ML of Fe.

Surprisingly, the [110] direction appears to be the easy-axis of magnetization also in the top FM film, as is seen from a comparison between the loops measured along [110] and [100] directions and shown in figure 4. When hysteresis loops are taken along the [100] direction (figure 4(*b*)), the coercivity in the top FM film is higher than the one measured along [110] (figure 4(*a*)). The same effect concerns the bottom Fe film, but is less visible due to the scale of the figure. It means that the uniaxial magnetic anisotropy, characteristic of Fe films grown on GaAs(001) [12–14], persists in the top FM film in spite of the MgO barrier, suggesting that this anisotropy is related to the growth-induced film morphology.

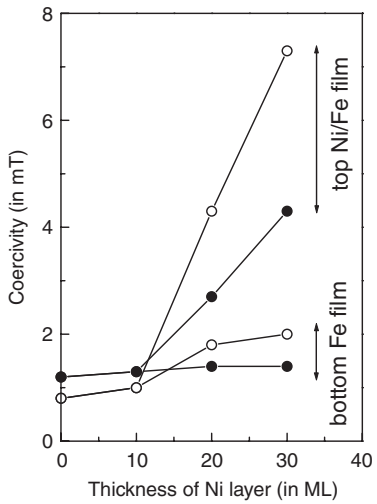

Figure 3. Coercivity of bottom Fe film and top Ni/Fe bilayer of Ni/6 ML Fe/10 ML MgO/14 ML Fe (○) and Ni/10 ML Fe/10 ML MgO/14 ML Fe (●), grown on GaAs(001), plotted vs the Ni layer thickness. The influence of the covering Ni layers on the coercivity is less pronounced when the top Fe film is thicker.

The magnetic hardening by Ni, however, does not solely affect the top Fe layer, but also the bottom layer shows changes of the coercivity. The net ellipticity of the junction, as it is seen from our MOKE loops measured for completed junction structures, does not correspond to the balance between the magnetization of both FM films when the total thickness of the junction approaches the penetration depth of the laser light (it is known that the Kerr signal is more sensitive to the outer layers). This is why with increasing total thickness of the structure, the contribution of the bottom Fe film is less visible. This effect is shown in figure 5, which includes both the loop of the single 14 ML thick Fe film deposited on GaAs(001) and the loop of the softer layer measured for the complete junction (i.e. for the maximum field around the coercivity field corresponding to the magnetization switching in the bottom 14 ML thick Fe layer of the junction). The difference between the loops concerns the ellipticity (as mentioned above) as well as the coercivity that is increased (as it is also seen, e.g. in figures 2(*a*)–(*c*)). The loop measured for the complete structure with the maximum field around the coercivity of the bottom Fe layer reflects the magnetization reversal process in the bottom Fe film in the presence of the magnetically saturated top Ni/Fe bilayer. The loop is symmetric and barely shifted by 0.15 mT. This small shift shows that the bottom and top layers are magnetically decoupled, to be more precise, that there is no FM or anti-ferromagnetic coupling of reasonable size.

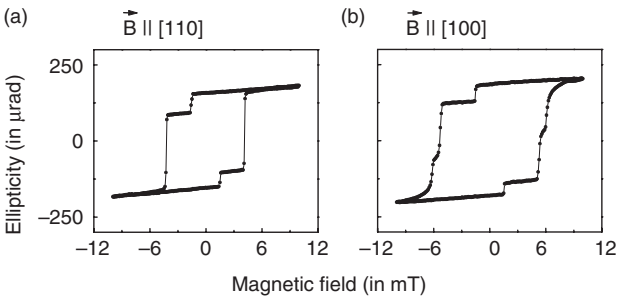

Figure 4. MOKE loops measured at RT for 30 ML Ni/10 ML Fe/10 ML MgO/14 ML Fe/GaAs(001): (*a*) along the [110], (*b*) along the [100] direction. The coercivity is higher when the loops are measured along the [100] direction confirming that the uniaxial magnetic anisotropy persists in the top FM film.

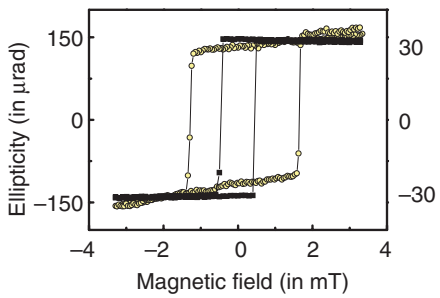

Figure 5. MOKE loops measured at RT along [110] for 14 ML of Fe: as the separate film on GaAs(001) (■, left axis) and as the bottom film building up the 30 ML Ni/10 ML Fe/10 ML MgO/14 ML Fe/GaAs(001) junction (○, right axis). The last one was measured for the maximum field around the coercivity corresponding to the magnetization switching in the bottom Fe film of the junction. The small shift between the loops shows that there is no ferro- or anti-ferromagnetic coupling between the bottom and top FM layers.

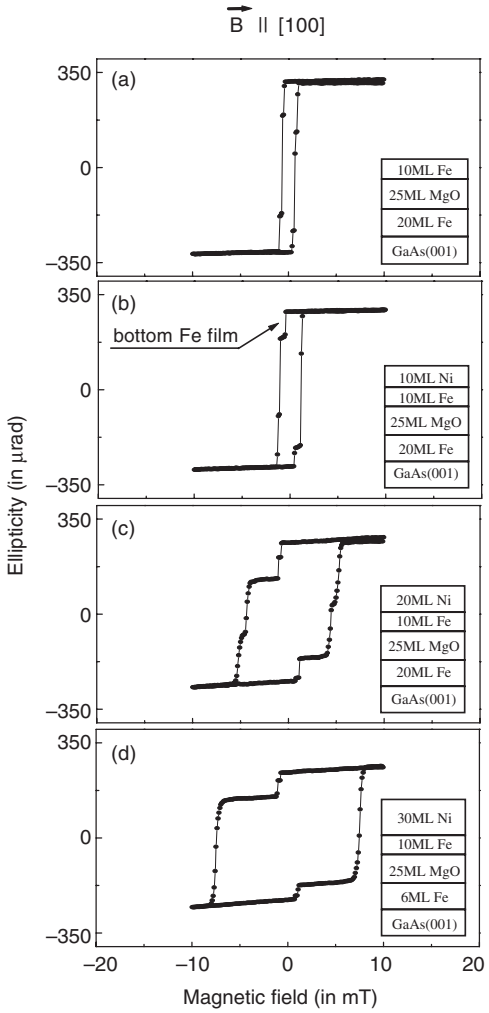

Figure 6. MOKE loops measured at RT along the [100] direction for 10 ML Fe/25 ML MgO/20 ML Fe/GaAs(001) (*a*), then covered with 10 ML of Ni (*b*), 20 ML of Ni (*c*) and 30 ML of Ni (*d*). The influence of the of the top FM film on the coercivity of the bottom one almost vanishes at a MgO thickness of about 25 ML.

The influence of the magnetic hardening of the top layer by Ni on the bottom Fe layer is a function of the MgO spacer thickness. From the shape of the hysteresis loops measured for junctions of varying MgO thickness, it is seen that the influence of the top FM film on the bottom one decreases fast with increasing MgO thickness, and almost vanishes above about 25 ML of MgO. The coercivities approach the values of single films irrespectively of the Ni layers. This is clearly deduced from the unchanged coercivity in the bottom Fe film after the junction structure was completed, as it is observed from figures 6(*b*)–(*d*) in comparison to figure 6(*a*).

The hysteresis loops we measured for Ni/Fe/MgO/Fe junctions grown on InP(001) show simultaneous switching of magnetization in both FM layers. After the deposition of the first (bottom) Fe film, the uniaxial magnetic anisotropy with the easy-axis of magnetization along the [−110] direction is clearly visible (figures 7(*a*) and (*b*)). Taking into account the lack of LEED pattern and the disordered structure seen in the TEM cross-section, the nature of the uniaxial in-plane magnetic anisotropy remains unclear. After the deposition of the MgO insulating barrier and the top Fe film (10 ML thick),

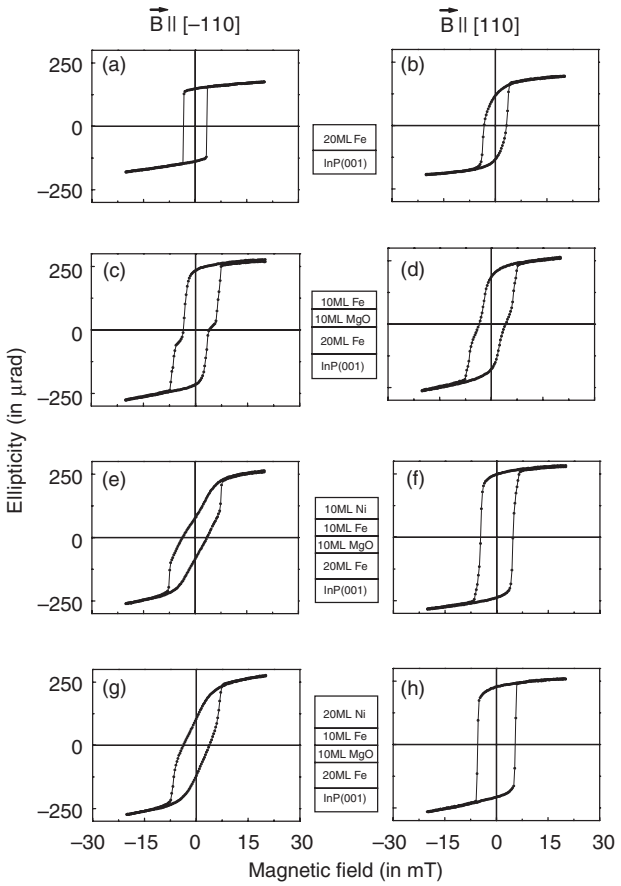

Figure 7. MOKE loops measured at RT along the [−110] and [110] directions, for 20 ML Fe/InP(001) ((*a*) and (*b*), respectively), for 10 ML Fe/10 ML MgO/20 ML Fe/InP(001) ((*c*) and (*d*), respectively), then covered with 10 ML of Ni ((*e*) and (*f*), respectively) and 20 ML of Ni ((*g*) and (*h*), respectively). Applying the magnetic field along the [110] direction, the switching of magnetization in both FM films occurs at the same magnetic field suggesting ferromagnetic coupling of the two films.

two-step loops were measured, but of only slightly different coercivity for both films (figures 7(*c*) and (*d*)). Assuming that the steps correspond to the coercivity of the bottom and top Fe films, the almost identical coercivity is not surprising. After an additional covering of the top Fe film with 10 ML of Ni (figures 7(*e*) and (*f*)) or more (figures 7(*g*) and (*h*)), the loops become one-step-like. Applying the magnetic field along the [110] direction, the switching of magnetization in both Fe films occurs at the same magnetic field corresponding to the average coercivity of both FM films weighted with their total magnetic moment. This points at FM coupling of the two layers.

4. Discussion

The coercivity corresponding to the magnetization reversal in the bottom Fe film in the structure differs from the coercivity of an individual Fe film of the same thickness. This effect is usually related to the coupling energy between both FM films building up the structure. The magnetic coupling between two FM films can originate in several effects [11]: (a) pinholes across the insulating barrier, (b) 'orange-peel' coupling resulting from the roughness of magnetic electrodes

and (c) coupling between the domain walls by stray fields from walls in FM films.

Pinhole formation and the resulting metallic 'bridges' should be immediately reflected in an electrical short-circuit between the FM electrodes, which we excluded with conductivity measurements (not shown). In addition, the FM coupling should be strong in this case and visualized by the strong dependence of the coercivity of the bottom Fe film on the MgO thickness [18], which is not the case. In particular, the switching field of the bottom Fe film should be sensitive to the magnetization of the top FM film and increase with the magnetization of the top layer. The tendency we observe (see figure 3), however, is quite opposite.

Orange-peel coupling is negligible because the interfaces are very sharp (figure 1(*a*)) and spreads over no more than 2–3 ML. Furthermore, any FM coupling should lead to a shifted loop for the bottom layer, if measured around the coercivity field of the bottom Fe layer, which we excluded (see figure 5).

The coupling between the domain walls cannot play any crucial role. In this thickness range, we are close to the single-domain limit that is also supported by the shape of the hysteresis loops we measured. The loops measured along the easy-axis of magnetization are of regular rectangular shape characterized by sharp magnetization switching. The magnetization reversal does not occur continuously within a certain range of the increasing magnetic field [19]. The loops suggest that no dipolar coupling between the domain walls exists: after the magnetization in the bottom Fe film is abruptly switched, the loops continue almost ideally parallel to the field axis. Only when the coercivity of the top layer is reached, it switches abruptly from the anti-parallel orientation with respect to the bottom layer to the parallel configuration.

Nevertheless, the switching fields display a strong dependence on the thickness of the top FM films and a weaker one on the MgO insulating barrier. However, the increase of the coercivity in the bottom Fe film is related rather to the thickness of the Ni layer than to the magnetization of the top Ni/Fe film. As it is shown in figure 3, the coercivity of the bottom Fe film is slightly affected by the top FM film, and even less affected when the magnetization of the top Ni/Fe film is increased by a thicker Fe layer. In addition, adding 10 ML of Fe to the Ni/Fe bilayer (that clearly decreases its coercivity) does not influence the coercivity of the bottom Fe film (figure 2(*d*)). This indicates that the coercivity of the bottom layer is not directly related to the magnetic moment or coercivity of the top layer. Also the negligible FM coupling between the films (see figure 4) supports that the magnetic hardening of the bottom layer is not driven by any kind of magnetic coupling to the top layer. Instead, it suggests that the top FM layer affects the coercivity of the bottom one by changing its crystallographic structure. Crystallographic defects like dislocations created in the top Ni/Fe film might be transmitted through the MgO to the bottom film as it is a common process in the single-crystalline structure. This suggestion is based on an irreversible character of the changes of the bottom Fe film coercivity, that are not related to the maximum moment and the maximum coercivity of the top Ni/Fe layer. With increasing the thickness of Ni grown on the bcc-Fe, its lattice transformation to the transformed-bcc [17] structure must result in an increasing number of defects. The structural defects cause the increase of the coercivity of the top Ni/Fe film, and possibly simultaneously penetrate into the bottom Fe film increasing its coercivity as well (figure 3). If the Fe layer in the top Ni/Fe film is thicker, then it is less susceptible for the Ni layer lattice transformation. As a result, the coercivity of the bottom Fe film increases only slightly with adding Ni to the top film. The growth of 10 ML of Fe on the top Ni/Fe does not create any new defects, thus the coercivity of the bottom Fe film remains unchanged (figure 2(*d*)). The influence of the top FM film on the bottom one decreases fast with increasing the MgO thickness and vanishes above the thickness of about 25 ML (figure 6). This was deduced from the fact that the coercivity fields approach the values of separated films. In this case, the MgO layer is thick enough that the crystallographic defects created in the top Ni/Fe cannot reach the bottom Fe film and affect its coercivity. This is in agreement with what one can expect by a qualitative analysis of the strains existing in the Ni/Fe/MgO/Fe single-crystalline system grown on GaAs(001). The lattice constants of Fe (2.87 Å) and MgO (4.21 Å, MgO[110]‖Fe[100]) are smaller in comparison to the lattice constant of GaAs(001) (1/2 of 5.65 Å), thus both the bottom Fe and MgO layers (pseudomorphically grown on GaAs(001) and on Fe, respectively) are compressed. In the case of very thin MgO layer, the stress is not relaxed and the growth of the top Fe layer proceeds almost in the same way as of the bottom one. In the case of thick MgO layer, the stress is relaxed, thus the top Fe layer is expanded to fit the lattice constant of the 'bulk' MgO, and thus less sensitive to the structural transformation occuring in the forthcoming Ni overlayer.

Note that in the loops measured along the [100] direction (that is the four-fold easy-axis of magnetization), the magnetization reversal process in the top Ni/Fe bilayer occurs in two steps, which are characterized by two slightly different coercivities (figures 4(*b*) and 6(*c*)). The simplest interpretation relates the steps to successive switching of magnetization by 90° domain walls. This is supported by the symmetry of the steps.

The MgO barrier in the structures grown on GaAs(001) appears continuous and pinhole-free at the TEM scale. This correlates with the observed independent switching of magnetization and the negligible FM coupling between both FM layers. In the case of Ni/Fe/MgO/Fe structures grown on GaAs(001), due to the almost perfect structural quality, continuity and flatness of the MgO film, both FM films are electrically insulated. On the other hand, the MgO barrier in the Ni/Fe/MgO/Fe structure grown on InP(001) is of worse quality as it is visible first of all from its 'wavy' interface (compare figures 1(*b*) with (*a*)). Such an interface may be responsible for the strong FM coupling between the top and bottom FM layers observed in this case [11]. The strong magnetic coupling is deduced from the hysteresis loops we measured for Ni/Fe/MgO/Fe junction structures grown on InP(001). We attribute this behaviour to the wavy interfaces in the junction in this case. Such rough features ('orange-peel') at the interfaces of the bottom Fe film are reproduced in the MgO interface with the top FM film (figure 1(*b*)) and magnetostatic coupling occurs between them. The coupling causes the simultaneous switching of magnetization in both FM films.

It is clearly seen from figures 7(*a*) and (*b*) that the Fe film deposited on InP, despite its polycrystalline structure, exhibits an in-plane anisotropy. The [−110] direction seems to be the easier axis of magnetization in comparison to the [110] axis very likely due to the morphology of the film that reflects the InP(001) reconstruction [12]. In addition, by covering the top Fe film with Ni, the in-plane anisotropy is changed in both FM films of the Ni/Fe/MgO/Fe/InP(001) structure. The [110] direction becomes the common easy-axis of magnetization of the structure, whereas [−110] seems to be a hard-axis of magnetization, in particular for the bottom Fe layer (figure 7). A similar observation was made for Fe films grown on InP(001): above a critical thickness of about 20 ML of Fe, the [110] direction became the easier axis of magnetization with no correlation to the film morphology as seen by STM. A structural transformation of the films is suggested to be responsible for this changed in-plane magnetic anisotropy of the system in both cases. However, this statement is difficult to be proven due to the film structure which is polycrystalline and no LEED analysis can be performed. Also the STM experiments were not able to detect a clear change in the morphology of such a disordered system.

5. Summary

In the case of single-crystalline Ni/Fe/MgO/Fe/GaAs(001) structures grown on GaAs(001), MOKE analysis confirms that the steps in the hysteresis loops correspond to magnetization reversal processes that occur independently in both FM films. The loops measured for the bottom Fe films (for the maximum field around the coercivity of the separate film of the same thickness), in the presence of the top Ni/Fe film, are symmetric around zero field showing that the films are not ferromagnetically coupled. The loops measured along [110] (easy-axis of magnetization) are of rectangular shape, showing sharp magnetization reversals and the anti-parallel orientation of magnetization in the two FM layers in a well-defined range of the applied field. The coercivity in the bottom Fe film increases with the increasing thickness of Ni layer in the top Ni/Fe film. We suggest that this fact is caused by the crystallographic defects created in the top Ni/Fe bilayer that penetrate the bottom Fe film.

For magneto-tunnel structures grown on InP(001), a strong FM coupling between the FM films is deduced from the hysteresis loops showing simultaneous switching of magnetization in both films. This behaviour is interpreted as a result of orange-peel coupling.

References

[1] Zhu H J, Ramsteiner M, Kostial H, Wassermeier M, Schonherr H-P and Ploog K H 2001 *Phys. Rev. Lett.* **87** 016601
[2] Schmidt G, Ferrand D, Molenkamp L W, Filip A T and van Wees B J 2000 *Phys. Rev.* B **62** R4790
[3] Rashba E I 2000 *Phys. Rev.* B **62** R16267
[4] Hanbicki A T, Jonker B T, Itskos G, Kioseoglou G and Petrou A 2002 *J. Appl. Phys.* **80** 1240
[5] Hu C-M and Matsuyama T 2001 *Phys. Rev. Lett.* **87** 066803
[6] Moodera J S and Mathon G 1999 *JMMM* **200** 248
[7] Butler W H, Zhang X-G, Schulthess T C and MacLaren J M 2001 *Phys. Rev.* B **63** 054416
Zhang X-G and Butler W H 2001 Private communication
[8] Mathon J and Umerski A 2001 *Phys. Rev.* B **63** 220403(R)
[9] Bowen M *et al* 2001 *Appl. Phys. Lett.* **79** 1655
[10] Rippard W H and Buhrman R A 2000 *Phys. Rev. Lett.* **84** 971
[11] Platt C L, McCartney M R, Parker F T and Berkowitz A E 2000 *Phys. Rev.* B **61** 9633
[12] Zavaliche F, Wulfhekel W and Kirschner J submitted
[13] Xu Y B, Kernohan E T M, Freeland D J, Ercole A, Tselepi M and Bland J A C 1998 *Phys. Rev.* B **58** 890
[14] Przybylski M, Chakraborty S and Kirschner J 2001 *J. Magn. Magn. Matter.* **234** 505
[15] Zavaliche F, Przybylski M, Wulfhekel W, Grabowski J, Scholz R and Kirschner J 2002 *Surf. Sci.* **507–510** 560
[16] Wulfhekel W, Klaua M, Ullmann D, Zavaliche F, Kirschner J, Urban R, Monchesky T and Heinrich B 2001 *Appl. Phys. Lett.* **78** 509
Klaua M, Ullmann D, Barthel J, Wulfhekel W and Kirschner J 2001 *Phys. Rev.* B **64** 134411
[17] Heinrich B, Celinski Z, Konno H, Arrott A S, Ruhrig M and Hubert A *Mater. Res. Symp. Proc.* **313** 485
[18] Keavney D J, Fullerton E E and Bader S D 1997 *J. Appl. Phys.* **81** 795
[19] Yu C C and Petford-Long A K 1999 *J. Appl. Phys.* **85** 5753